

# Generative Modeling of Approximately Periodic Time Series by a Posterior-Weighted Gaussian Process

Elias Reich<sup>[0009–0000–4561–9067]</sup>, Saverio Messineo<sup>[0000–0003–1592–4428]</sup>, and  
Stefan Huber<sup>[0000–0002–8871–5814]</sup>

Josef Ressel Centre for Intelligent and Secure Industrial Automation  
Salzburg University of Applied Sciences, Salzburg, Austria  
`eliassteffen.reich@fh-salzburg.ac.at`

**Abstract.** Discrete automated processes in industrial and cyber-physical systems often exhibit a repetitive structure in which successive repetitions follow a common trajectory while differing in duration, amplitude, and fine-scale dynamics. Such *approximately periodic* behavior poses a challenge for Gaussian Processes (GP) modeling: strictly periodic models suppress inter-repetition variability, while non-periodic models fail to capture the strong structural regularities required for generation. In this work, we propose a stochastic generative model for approximately periodic time series. The model is based on a GP whose posterior is modulated by a novel kernel. Our approach decouples intra-repetition structure from inter-repetition variability through a two-stage construction which yields a generative distribution with a identical mean function across repetitions, while allowing smooth variation between repetitions. The modeling choices are supported by an implementation in which realistic synthetic trajectories are generated from toy datasets.

## 1 Introduction

Discrete automated processes, such as those encountered in industrial production machines, robotic assembly lines, and cyber-physical control systems, often exhibit a characteristic form of repetition. Due to sensor noise, mechanical wear, environmental fluctuations, and control variability, such processes are not strictly periodic. Still, their observable dynamics consist of successive iterations that are similar in shape and duration. As a result, measurements collected during operation give rise to multivariate time series that repeatedly traverse comparable trajectories while exhibiting non-negligible variation across repetitions. In this setting, Gaussian Processes (GPs) [14] are an appealing model: they provide a principled probabilistic model with calibrated uncertainty and interpretable structure, and periodic or quasi-periodic kernels allow us to encode repetition while retaining flexibility for repetition-to-repetition variability. The task of this paper is to propose a novel, stochastic generative model based on the GP, that formalizes and reproduces processes whose iterations “nearly” repeat themselves.

To the best of our knowledge, no prior GP-based generative model provides: (i) long-horizon generative stability across arbitrarily many repetitions, and (ii) controlled, smoothly decaying inter-repetition variability. Our kernel-modulated posterior addresses this gap and is practically relevant in several application domains: it enables the generation of realistic synthetic data for unit testing, digital twins or populating honeypots in industrial systems; and it naturally supports likelihood-based anomaly detection by quantifying deviations from learned statistics.

*Problem formulation.* Formally, observations of systems with repetitive behavior can be characterized as multivariate time series over a finite interval

$$x: I \rightarrow \mathbb{R}^D \quad \text{with} \quad I = [0, N] \subset \mathbb{R},$$

that can be decomposed into consecutive segments  $I_1, I_2, \dots, I_r$ , with  $\bigcup_j I_j = I$  and each interval  $I_j$  corresponding to an individual repetition of the underlying process. We do not require that the  $I_j$  have equal length. By introducing reparameterizations  $\pi_i: I_i \rightarrow [0, 1]$  that normalize time, we define the *time-normalized repetition* as  $y_i(t) = x(\pi_i^{-1}(t))$  for all  $t \in [0, 1]$ . Given  $\varepsilon > 0$ , we call  $x$  *repetitive* and, in turn,  $y_1, \dots, y_r$  repetitions of an *approximately periodic* time series, if and only if  $\|y_i - y_j\|_\infty \leq \varepsilon$  for all  $1 \leq i, j \leq r$ . In such a case, a pair  $(y_i, y_j)$  is called *approximately equivalent*. The process of splitting  $x$  in its repetitions is shown in [10]. To keep the proposed method as streamlined as possible, we will from now on assume that all time series data are already split into their repetitions and reparametrized to satisfy the constraints for approximate periodicity. Avoiding notational clutter, we will say  $y$  is a vector which contains all repetitions in order  $[y_1, \dots, y_r]^\top$  and  $T$  is the vector of their respective domains  $[T_1, \dots, T_r]^\top$ . We will also assume  $D = 1$ , but the model can be employed in higher dimensions through multi-output GPs such as the linear model of coregionalization (LMC) [1].

Generating approximately periodic processes poses a challenge for GP models. Classical periodic models enforce exact repetition and therefore fail to represent realistic inter-repetition variability, while generic non-periodic models disregard the strong structural regularities present in the data and therefore fail to make long term predictions. From a generative modeling perspective, this is particularly limiting: the model should be capable of producing arbitrarily long sequences of repetitions that preserve the characteristic shape of the process, while allowing variation between repetitions.

*Contributions.* In this paper, we introduce a stochastic generative model for *approximately periodic* multivariate time series based on GPs, that can generate time series of arbitrarily many repetitions, preserving continuity over the whole time span while still allowing variation between repetitions. Our approach consists of two conceptually separate stages: (1) learning a stable repetition template using a strictly periodic GP posterior, and (2) injecting controlled variability between repetitions by modulating the posterior covariance with a smooth

envelope. This separation ensures that the model’s mean dynamics remain consistent across arbitrarily long horizons, while its covariance structure reflects the natural decay of similarity between repetitions. This yields a generative model that produces trajectories with identical mean structure across repetitions while allowing smooth variation between repetitions.

## 2 Related Work

Periodic kernels and their quasi-periodic variants are long-standing tools for modeling repetitive structure in time series [14]. In astronomy and astrophysics, scalable one-dimensional GP methods enable quasi-periodic modeling of stellar rotation and activity over long light curves [3]. Recent analyses connect quasi-periodic kernel hyperparameters to physically meaningful timescales and study their identifiability and sampling effects [7]. While effective and efficient algorithms for forecasting and uncertainty estimation exist [3, 4, 6], these methods either enforce exact periodicity or introduce mean decay and variance inflation over long horizons, limiting their use as *generative* models for arbitrarily many repetitions.

A substantial line of work recasts temporal GP regression as linear state-space models, yielding  $\mathcal{O}(N)$  inference via Kalman filtering and smoothing, with explicit linkages for periodic/quasi-periodic covariances [11]. These methods improve scalability and bring physical insight, but they do not by themselves enable long-horizon generation.

Neural ODEs [2] and diffusion/score-based models [12] achieve impressive generative performance but often trade off interpretability and calibrated uncertainty as well as long-term stability [9]. For safety-critical industrial and cyber-physical applications, where stability is central, GPs remain attractive.

## 3 Methodology

We refer to the standard textbook [14] on GPs. Below we give a short GP primer to introduce the notation used throughout the paper. Let training inputs be  $T = [t_1, \dots, t_n]^\top$  with observations  $y = [y_1, \dots, y_n]^\top$  and define a positive-semi-definite (PSD) kernel/covariance function  $k(t, t')$  with Gram-matrix  $K$ . Evaluated on the training inputs  $K := K(T, T)$ , the matrix has entries  $[K]_{ij} = k(t_i, t_j)$ . For a test input  $t_*$  we write  $k_* := K(T, t_*)$  for the cross covariances and  $k_{**} := K(t_*, t_*)$  for the covariances. If there are multiple test inputs, we refer to them as  $T_*$ . With i.i.d. Gaussian observation noise  $\epsilon \sim \mathcal{N}(0, \sigma^2 I)$  and prior over the latent (unobserved, noiseless) function  $f \sim \mathcal{GP}(\mu, k)$  – in practice the mean function  $\mu$  is usually zero without loss of generality – the standard posterior (i.e., predictive) distribution at  $t_*$  is available in closed form:

$$\begin{aligned}
 f(t_*) \mid T, y &\sim \mathcal{N}(\hat{\mu}, \hat{\Sigma}) \quad \text{with} \\
 \hat{\mu} &= \mu(t_*) + k_*^\top (K + \sigma^2 I)^{-1} (y - \mu(T)), \\
 \hat{\Sigma} &= k_{**} - k_*^\top (K + \sigma^2 I)^{-1} k_*.
 \end{aligned} \tag{1}$$

Throughout this paper, we will rarely consider univariate inputs and outputs, if so it is explicitly stated; otherwise  $T = [T_1, \dots, T_r]^\top$  will denote the inputs for  $r$  repetitions  $y = [y_1, \dots, y_r]^\top$ .

The core modeling challenge is to obtain a GP posterior that is approximately periodic in the sense that

- (i) the posterior mean is identical across repetitions, and
- (ii) the posterior covariance permits variation between repetitions.

A prior for periodic processes with period length  $p$ , kernel width  $l_\theta$  and signal variance (average distance from the prior mean)  $\sigma_f^2$ ; is an exponential kernel with inputs embedded on the circle [14]. We will consider  $\theta = (l_\theta, \sigma_f^2, \sigma_\theta^2)$ , where  $\sigma_\theta^2$  is the prior noise variance from (1), as optimizable hyperparameters. The periodic kernel can be written as

$$k_\theta(t, t') = \sigma_f^2 \exp\left(\frac{2}{l_\theta^2} \sin\left(\frac{\pi}{p}(t - t')\right)^2\right). \quad (2)$$

Under this prior, the posterior predictive mean is exactly periodic, and both variances and covariances repeat identically at integer multiples of the period duration  $p$ . Consequently, uncertainty is propagated forward without attenuation: predictions at arbitrarily large horizons exhibit the same uncertainty as predictions near the observed data. This behavior is often undesirable in regression settings, where uncertainty is typically expected to grow. For generative modeling however, this behavior is beneficial. A generative model is expected to reproduce the empirical statistics of the data indefinitely; enforcing increasing uncertainty over time would eventually destroy the characteristic structure of the generated trajectories.

An additional property of the periodic kernel is that for grid-sampled data (all  $r$  repetitions obtained as a sequence with equal sampling distances) the joint covariance across the concatenated observations has a block structure: the diagonal blocks equal  $K + \sigma^2 I$  (the per-repetition covariance matrix plus observation noise) and every off-diagonal block equals the shared covariance matrix  $K$ . This block structure simplifies algebra and enables the following strong statement about the predictive mean:

*Property 1.* If data is sampled on a grid then the posterior mean evaluated on the grid will converge to the empirical mean as the observation noise  $\sigma^2 \rightarrow 0$ . Computing the posterior mean and covariance on  $r$  repetitions is equivalent to computing them on one repetition, scaling  $\sigma^2$  by  $\frac{1}{r}$  and replacing  $[y_1, \dots, y_r]^\top$  by the mean repetition  $\frac{1}{r} \sum_{i=1}^r y_i$ .

*Proof.* The proof is deferred to the appendix section 5.1.

Although property 1 was derived under the assumption of repeated observations on a fixed grid, it provides useful intuition for more general settings. In

particular, it shows that a GP with a periodic kernel naturally encodes variability between repetitions through the noise parameter  $\sigma^2$ . Because the periodic kernel maps phase-aligned inputs from different repetitions to the same points in feature space, the model effectively receives multiple (potentially different) observations at those same locations. Any mismatch between these repeated values must then be explained by the observation noise, and is therefore captured in  $\sigma^2$ .

To relax strict periodicity, we introduce a smoothly decaying correlation envelope  $w$  with hyperparameters  $\psi = (l_\psi, \sigma_\gamma^2)$  that decreases the covariance between repetitions:

$$w_\psi(t, t') = \sigma_\gamma^2 \exp\left(-\frac{\|\phi(t) - \phi(t')\|^2}{2l_\psi^2}\right) \quad \text{with} \quad \phi(t) = \int_0^t \sin\left(\frac{\pi}{p}\tau\right)^2 d\tau. \quad (3)$$

The kernel  $w$  is a Gaussian kernel in an embedding space, which has vanishing derivatives at integer multiples of  $p$  to avoid unwanted phase shifts in the weighted kernel  $g = w \cdot k$ . Intuitively, the mapping stretches and contracts the time axis in a way that preserves periodic structure but gradually attenuates long-range interactions, Figure 1 illustrates the shift in local covariance maxima.

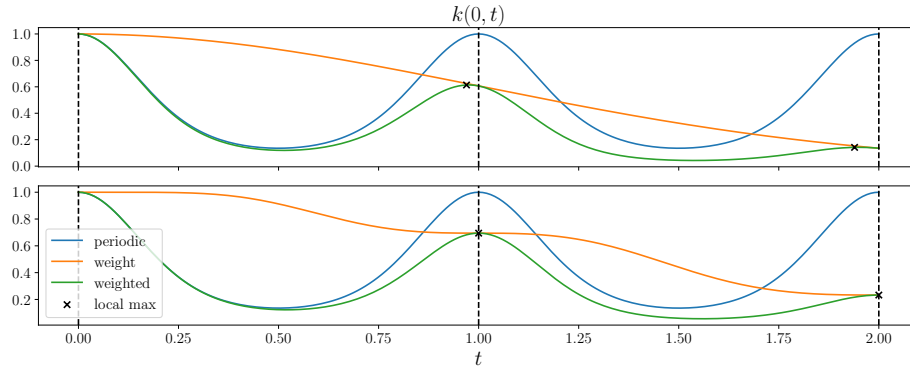


**Fig. 1.** The top row shows the periodic kernel  $k_\theta$  and squared exponential kernel (weight) over two periods ( $p = 1$ ) as well as the product of the two kernels (weighted), all centered around 0. The bottom figure replaces the standard squared exponential kernel with the proposed weight  $w_\psi$ .

Naively using  $g$  as a prior will have the effect of a decaying posterior mean  $\hat{\mu}$  and increasing posterior variances  $\sigma^2 = \text{diag}(\hat{\Sigma})$ , see fig. 2. To illustrate this behavior, consider the single point prediction at test inputs  $t^*$  given observations

$(T, y)$  [14]:

$$\begin{aligned}
 p(f(t^*)|T, y) &= \mathcal{N}(\hat{\mu}, \hat{\Sigma}) \quad \text{with} \\
 \hat{\mu} &= g(T, t^*)^\top g(T, T)^{-1} y = \sum_i g(T_i, t^*) g(T, T)_{i,:}^{-1} y, \\
 \hat{\Sigma} &= g(t^*, t^*) - g(T, t^*)^\top g(T, T)^{-1} g(T, t^*) \\
 &= g(t^*, t^*) - \sum_{i,j} g(T_i, t^*) g(T_j, t^*) g(T, T)_{i,j}^{-1}
 \end{aligned} \tag{4}$$

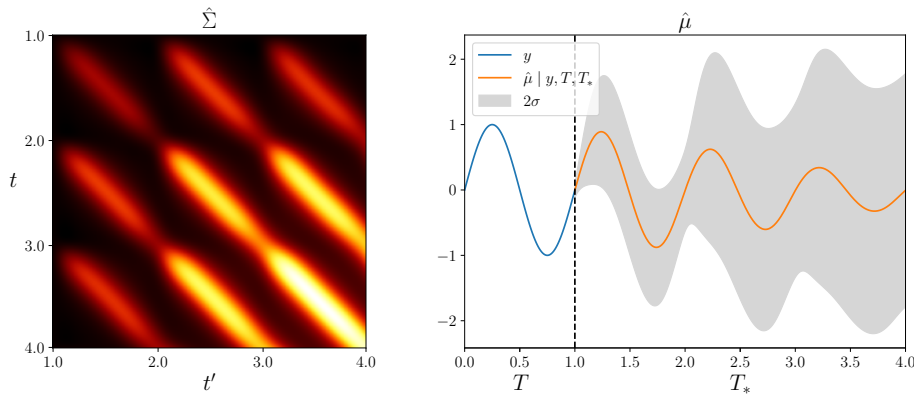


**Fig. 2.** Posterior covariance matrix  $\hat{\Sigma}$  and mean  $\hat{\mu}$  with a weighted periodic prior covariance at test locations  $T_*$ . Variances as well as covariances are increasing and the predictive mean decays.

In the mean expression in (4), observe that the quantity computed is simply a weighted sum of the values in the weighted periodic covariance matrix  $g(T_i, t^*)$ . As the difference  $|T_i - t^*|$  increases, the covariance tends to zero. The predictive mean will thus decay to the prior (zero-) mean function, violating condition (i). For the predictive covariances the quadratic term will vanish for small  $|T_i - t^*|$  and thus tends to  $g(t^*, t^*)$ , i.e., the maximum value the covariance matrix can take, hence violating condition (ii). Thus, a periodic kernel with decaying envelope implies a posterior with decaying mean and increasing variances. To avoid this pathology, we decouple the intra- and inter-repetition statistics by adopting a two-stage construction.

### 3.1 Stage 1: Periodic prior GP

In the first stage, we model the intra-repetition statistics using a strictly periodic GP prior,

$$y(t) = f(t) + \epsilon, \quad f \sim \mathcal{GP}(0, k_\theta(\cdot, \cdot)), \quad \epsilon \sim \mathcal{N}(0, \sigma_\theta^2), \tag{5}$$

and compute the posterior  $f_* \mid y \sim \mathcal{N}(\hat{\mu}_\theta, \hat{\Sigma}_\theta)$ . This stage yields an exactly periodic posterior.

Even though approximately periodic time series data typically consists of a single long trajectory, we will first interpret the observed repetitions  $y_1, \dots, y_r$  as (partially) independent realizations  $f_1, \dots, f_r$  of the same underlying periodic process,

$$\forall i \in \{1, \dots, r\}: y_i(t) = f_i(t) + \epsilon, \quad t \in T_i \quad (6)$$

where  $f_i \sim \mathcal{GP}(0, k_\theta)$  are independent draws of the latent function sharing common hyperparameters. However, a caveat of the fully factorized likelihood implied by independence is that the noise variance  $\sigma_\theta^2$  is not identifiable from individual repetitions. To mitigate this issue while retaining computational tractability, we adopt a mini-batched training strategy in which the negative log-likelihood (NLL) is evaluated over small batches  $\mathcal{B}$  of multiple repetitions. By jointly evaluating the kernel on the inputs of several repetitions, the likelihood  $\theta \mapsto \mathcal{N}(y \mid \theta)$  has to explain these variations, thereby stabilizing the estimation of the noise variance

$$\arg \min_{\theta} \sum_{\substack{y_{\mathcal{B}} \subseteq y \\ T_{\mathcal{B}} \subseteq T}} -\log \mathcal{N}(y_{\mathcal{B}} \mid 0, K_\theta(T_{\mathcal{B}}, T_{\mathcal{B}}) + \sigma_\theta^2 I). \quad (7)$$

Hyperparameter optimization yields a variance estimate that captures the intrinsic variability of the underlying process. During posterior construction, however, repetitions must be treated as observations of the same latent function in order to preserve the global spatial structure of the trajectory across repetitions. When using a periodic kernel, conditioning on multiple repetitions results in an unintended accumulation of evidence, which leads to an artificial attenuation of posterior uncertainty (eq. (13)). To compensate for this effect, we rescale  $\sigma_\theta^2$  by the effective number of repetitions after training. This adjustment restores uncertainty levels consistent with those identified during hyperparameter optimization.

### 3.2 Stage 2: Posterior weighting

In the second stage, inter-repetition correlations are introduced *after conditioning* by modifying the posterior covariance. Rather than altering the GP prior or kernel, we model these dependencies directly at the level of the posterior distribution. Using the weight kernel  $w_\psi$  only at the posterior stage preserves exact periodicity of the mean, while avoiding pathological behavior of weighted periodic priors, which cause mean decay and variance inflation. This choice is essential for maintaining long-horizon stability. Specifically, we define the following generative model:

$$\gamma \sim \mathcal{N}(\hat{\mu}_\theta, \Sigma_\psi := W_\psi \odot \hat{\Sigma}_\theta + \sigma_\psi^2 I), \quad (8)$$

where  $W$  is the kernel matrix induced by  $w_\psi$ , and  $\odot$  denotes elementwise multiplication (Schur product). We do not claim this construction defines a GP, i.e., no GP prior with this posterior exists. By construction,  $\gamma$  is a random variable,

specified at a finite set of evaluation points and follows a non-degenerate normal distribution, as the modified posterior covariance matrix is PSD by the Schur product theorem.

By leaving the posterior mean unchanged, the model enforces identical mean structure across all repetitions. By weighting the covariance, local uncertainty is preserved while ensuring that correlations between distant repetitions decay monotonically to zero. This behavior matches the statistical structure expected of approximately periodic data and avoids the degeneracies induced by envelope-weighted GP priors. An alternative construction, the additive combination of  $W$  and  $\hat{\Sigma}$ , is simpler from a modeling perspective but fails to eliminate long-range periodic correlations: once the envelope decays, the covariance matrix reverts to that of a strictly periodic GP posterior. The proposed multiplicative covariance modulation is therefore essential for suppressing long-range periodic correlations while preserving phase-aligned variance, resulting in a generative model whose second-order statistics more faithfully reflect those observed in approximately periodic data.

The strength of long range correlation dampening is decided by the length scale hyperparameter  $l_\psi$  of the weighting kernel and independent noise in the outputs is learned via the hyperparameter  $\sigma_\psi^2$ .<sup>1</sup> As in the single repetition model, we find their optima by NLL minimization. In contrast to the first stage, the observations  $y_1, \dots, y_r$  are now no longer treated as independent, as this would preclude inference on the inter-repetition correlations.

$$\arg \min_{\psi} (y - \hat{\mu}_\theta) \Sigma_\psi^{-1} (y - \hat{\mu}_\theta)^\top + \log \det \Sigma_\psi \quad (9)$$

We observe that the inverse and determinant term involving the Schur product ( $\Sigma_\psi$ ) admit no algebraic simplification. Evaluating the likelihood is thereby problematic with a large number of repetitions.

## 4 Experimental Setup

We evaluate the influence of the first-stage mini-batch size and the amount of output noise that the second stage must absorb. The dataset is a trajectory  $y_{\text{test}}(t_*)$ ,  $t_* \in T_*$  sampled from a weighted-periodic GP conditioned on the signal  $\sin(2\pi t)$ . From each of the 10 repetitions we pick 20 random points for training. Each stage is optimized via the two-stage NLL procedure; learned hyperparameters and mean squared error (MSE) between predictive and test mean  $\mu_{\text{test}}, \mu_\theta$  and pointwise standard deviations  $\hat{\sigma}_{\text{test}} := \sqrt{\text{diag}(\Sigma_{\text{test}})}$ ,  $\hat{\sigma}_\gamma := \sqrt{\text{diag}(\Sigma_\psi)}$  are reported for evaluation. The models are optimized using Adam (lr = 0.1) for 100 gradient steps in each stage<sup>2</sup>.

<sup>1</sup> This parameter also prevents a degenerate solution for the dampening ( $l_\psi \rightarrow 0$ ) in a noiseless setting. We recommend to discard  $\sigma_\psi^2$  after training if the generated trajectories need to be without noise.

<sup>2</sup> code available on <https://github.com/JRC-ISIA/2026-lion20-approx-periodic-gp-generative-model>

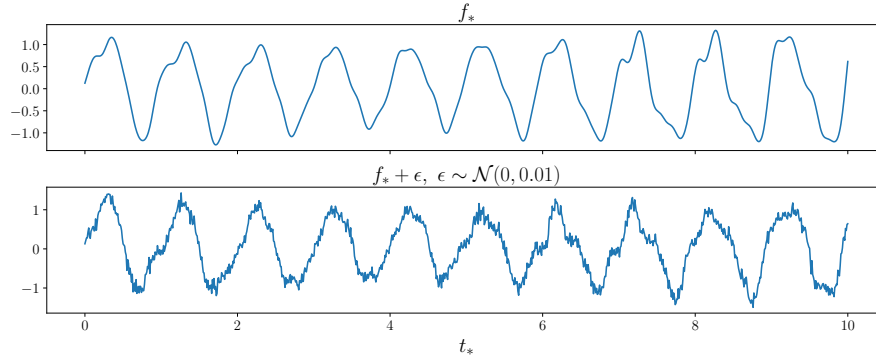


**Fig. 3.** Approximately periodic test data without noise (top) and with noise (bottom).

**Table 1.** Results on approximately periodic data with varying batch size  $|\mathcal{B}|$ .

$ \mathcal{B} $	$\text{MSE}(\mu_{\text{test}}, \mu_\gamma)$	$\text{MSE}(\hat{\sigma}_{\text{test}}, \hat{\sigma}_\gamma)$	$l_\theta$	$l_\psi$	$\sigma_\theta^2$	$\sigma_\psi^2$	$\sigma_f^2$	$\sigma_\gamma^2$
1	$1.88 \times 10^{-2}$	$2.45 \times 10^{-2}$	0.65	0.609	0.009	0.027	0.504	8.05
2	$1.34 \times 10^{-2}$	$4.33 \times 10^{-4}$	0.982	0.687	0.307	0.0	0.587	5.559
3	$1.36 \times 10^{-2}$	$1.04 \times 10^{-3}$	0.937	0.69	0.383	0.0	0.663	4.946
5	$1.27 \times 10^{-2}$	$2.13 \times 10^{-3}$	1.037	0.694	0.423	0.0	0.639	5.467
10	$1.31 \times 10^{-2}$	$1.93 \times 10^{-3}$	0.891	0.695	0.463	0.0	0.513	4.69

For noiseless approximately periodic data, we set the hyperparameters to  $l_k = 0.7, l_w = 0.8, \sigma^2 = 1.5$

$$\begin{aligned}
 y(t) &= f(t) + \epsilon, \quad f \sim \mathcal{GP}(0, k(t, t')w(t, t')), \quad \epsilon \sim \mathcal{N}(0, \sigma^2) \\
 y_{\text{test}}(t_*) &= f_*(t_*), \quad f_* \sim \mathcal{N}(\mu_{\text{test}}, \Sigma_{\text{test}}).
 \end{aligned}
 \tag{10}$$

For the second experiment, we add noise  $\sigma_{\text{out}}^2$  to the test data and fix the batch size  $|\mathcal{B}| = 2$ , as we see diminishing returns for larger numbers.

$$y_{\text{test}}(t_*) = f_*(t_*) + \epsilon_{\text{out}}, \quad \epsilon \sim \mathcal{N}(0, \sigma_{\text{out}}^2).
 \tag{11}$$

We also include results for periodic data, where we use the same hyperparameters and drop the weight kernel in the prior.

The final experiment follows a similar construction as the previous ones, but with 2-dimensional data. We condition on  $[\sin(2\pi t), -\sin(4\pi t)]$  and fit a LMC with non-stationary periodic kernel [8, 14]. The coregionalization matrix is optimized in the first stage. For details on multi-output GPs see [1].

#### 4.1 Discussion

The results in table 1 demonstrate a strong dependence of the first-stage variance estimates  $\sigma_\theta^2$  on the mini-batch size  $|\mathcal{B}|$ . When training with batch size

**Table 2.** Results on approximately periodic data with noise  $\sigma_{\text{out}}^2$  and  $|\mathcal{B}| = 2$ .

$\sigma_{\text{out}}^2$	$\text{MSE}(\mu_{\text{test}}, \mu_\gamma)$	$\text{MSE}(\hat{\sigma}_{\text{test}}, \hat{\sigma}_\gamma)$	$l_\theta$	$l_\psi$	$\sigma_\theta^2$	$\sigma_\psi^2$	$\sigma_f^2$	$\sigma_\gamma^2$
0.01	$1.35 \times 10^{-2}$	$3.85 \times 10^{-4}$	0.945	0.677	0.304	0.0	0.56	5.411
0.05	$1.48 \times 10^{-2}$	$3.97 \times 10^{-4}$	0.895	0.634	0.34	0.003	0.611	4.726
0.10	$9.63 \times 10^{-3}$	$4.87 \times 10^{-4}$	1.027	0.67	0.396	0.01	0.706	4.617
0.30	$1.11 \times 10^{-2}$	$9.06 \times 10^{-4}$	1.544	0.587	1.117	0.088	0.839	1.2
0.50	$2.53 \times 10^{-2}$	$1.78 \times 10^{-3}$	1.184	0.098	3.268	0.222	0.674	1.936

**Table 3.** Hyperparameters via minimizing the NLL on periodic data.

$ \mathcal{B} $	$l_\theta$	$l_\psi$	$\sigma_\theta^2$	$\sigma_\psi^2$	$\sigma_{\text{out}}^2$	$l_\theta$	$l_\psi$	$\sigma_\theta^2$	$\sigma_\psi^2$
1	0.922	0.959	0.003	0.0	0.01	0.801	0.902	0.002	0.0
2	0.816	0.917	0.001	0.0	0.05	1.082	1.405	0.033	0.003
3	0.819	0.913	0.001	0.0	0.10	1.909	1.021	0.106	0.01
5	0.758	0.907	0.001	0.0	0.30	2.247	0.824	0.902	0.084
10	0.679	0.906	0.001	0.0	0.50	1.623	2.081	2.726	0.27

$|\mathcal{B}| = 1$ , the estimated variance collapses towards zero, despite the fact that the observed repetitions exhibit substantial inter-repetition variability. As the batch size increases, the estimated variance stabilizes and approaches a non-degenerate value. This behavior reflects the fact that, under a strictly factorized likelihood, each repetitions are explained by independent latent functions. In this regime, the optimizer can reduce the NLL by ignoring variation, leading to systematic underestimation of  $\sigma_\theta^2$ . Evaluating the likelihood over mini-batches of multiple repetitions exposes the likelihood to inter-repetition variability, providing a stronger and more stable signal for estimating  $\sigma_\theta^2$  which results in better estimates for true pointwise variances  $\hat{\sigma}_{\text{test}}^2$ . The mean function  $\mu_{\text{test}}$  is correctly identified across all batch sizes and the learned hyperparameters are relatively consistent across all batch sizes  $|\mathcal{B}| > 1$ . See fig. 4 for a visual of the posterior with  $|\mathcal{B}| = 2$ .

The second experiment in table 2 illustrates the role of the posterior-weighting stage under noisy observations. Whereas the the additional diagonal variance  $\sigma_\psi^2$  in the weighting kernel was consistently driven to 0 in the noiseless setting, here its value is increasing with the additional noise put on the observations. For small noise levels we see that the first stage observation noise  $\sigma_\theta^2$  is barely changing, as the overall pointwise variation in the data is as high or higher than the perturbations. This behavior is then compensated by  $\sigma_\psi^2$ , and only for higher noise levels ( $> 0.1$ ), the first stage observation noise is increasing. This also explains why the signal variance  $\sigma_\psi^2$  is much smaller for these higher noise levels, as the parameter does not need to compensate the small variances from the first stage.

For comparison, table 3 (left half) reports results for strictly periodic data. In this setting, the batch size has no influence, which is to be expected as all repetitions are exactly equal. The posterior dampening parameter  $l_\psi$  is higher

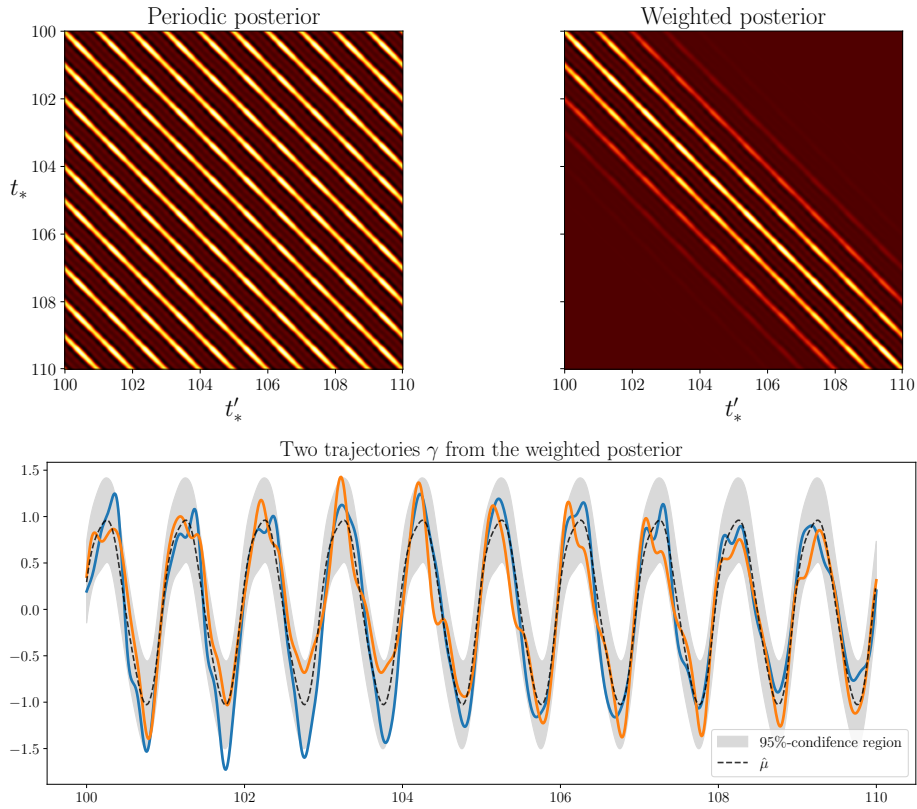


**Fig. 4.** Posterior covariance matrix and samples from  $\gamma$  with hyperparameters from the noiseless setting in table 1 with  $|\mathcal{B}| = 2$ .

as in the first example, but we have also seen much lower values in other experiments. Theoretically the optimum would be  $\infty$ , but with very low first stage prior variances  $\sigma_\theta^2$ , the posterior weighting has little to no effect, as the variation for trajectories  $\gamma$  is extremely low anyways. In the noisy setting table 3, the prior observation noise  $\sigma_\theta^2$  is a much better estimator for the true noise levels, as it is not responsible for also capturing the inter-repetition variation as well. The second stage noise variance  $\sigma_\psi^2$  is also reliably increasing with the noise level in the observations and all other hyperparameters are relatively consistent again.

The final experiment fig. 5 on a 2-dimensional dataset shows how our method is applicable to more complex problems than univariate, stationary time series. A periodic non stationary kernel in the first stage can find the varying degrees of variation in each cycle and project them forward indefinitely. This enables much more realistic trajectories, as naturally, the degree of variation is not the same

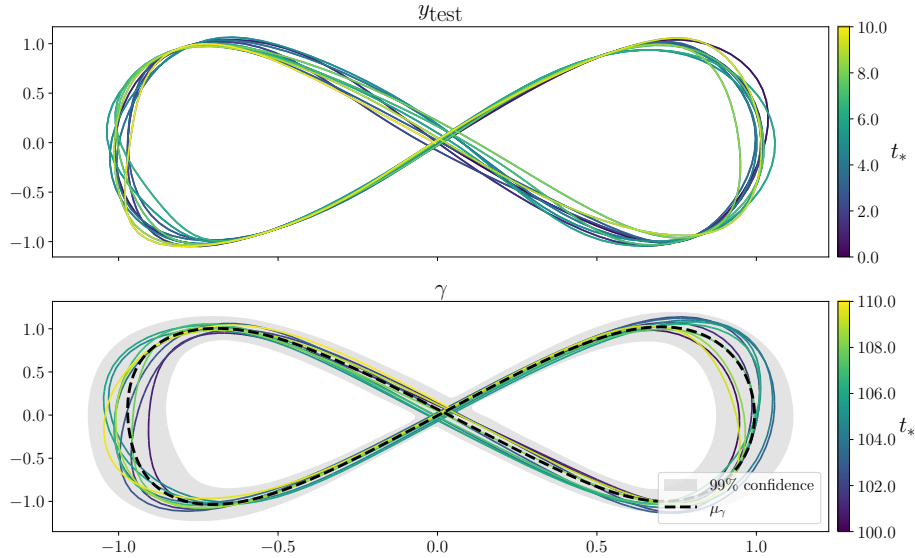


**Fig. 5.** Test data (top) and samples from  $\gamma$  (bottom). The non-stationary kernel can capture the high variance when crossing the origin from the second to the fourth quadrant.

everywhere. The second stage model decorrelation then introduces variation to the otherwise periodic trajectory.

Overall, the provided experiments highlight that mini-batch likelihood evaluation plays a crucial role in stabilizing variance estimation while keeping computational costs low in the first stage; and that the posterior weighting mechanism in the second stage provides a principled and effective means of modeling inter-repetition variability and output noise.

## 5 Conclusion

This paper demonstrates that modifying the GP posterior, rather than the prior, provides a principled way to model approximately periodic processes for generative purposes. The proposed model finds intra-repetition variability by assuming that the data are partially independent observations of a periodic GP prior. To enable the model to generate trajectories with variability, the posterior covariance of the periodic GP is modulated by a novel kernel which decorrelates repetitions, breaking the exact periodicity induced by the prior kernel. The resulting distribution is not a GP in the sense that it is the result of conditioning a GP prior, but a non-degenerate multivariate normal distribution derived from a GP posterior, from which trajectories of arbitrary length may be sampled. From an application perspective, the proposed model is well suited for synthetic data

generation of stationary processes which require stability and interpretability over long time spans.

Several directions for future work remain open. Scaling the likelihood optimization to large numbers of repetitions will require sparse or approximate inference techniques [5, 13], which could be adapted to the proposed covariance modulation framework. Extending the model to handle more complex repetition statistics and repetitive behavior could further improve expressiveness, which is inherently lacking in the proposed model, as is the case for all stochastic processes with unimodal posteriors. Finally, a systematic evaluation on real-world industrial datasets will be essential to quantify the practical benefits of the approach in downstream tasks such as anomaly detection and system simulation.

## References

1. Alvarez Mauricio A., L.R., Lawrence, N.D.: Kernels for vector-valued functions: A review. *Foundations and Trends® in Machine Learning* **4**(3), 195–266 (2012)
2. Chen, R.T.Q., Rubanova, Y., Bettencourt, J., Duvenaud, D.K.: Neural ordinary differential equations. In: Bengio, S., Wallach, H., Larochelle, H., Grauman, K., Cesa-Bianchi, N., Garnett, R. (eds.) *Advances in Neural Information Processing Systems*. vol. 31. Curran Associates, Inc. (2018), [https://proceedings.neurips.cc/paper\\_files/paper/2018/file/69386f6bb1dfed68692a24c8686939b9-Paper.pdf](https://proceedings.neurips.cc/paper_files/paper/2018/file/69386f6bb1dfed68692a24c8686939b9-Paper.pdf)
3. Foreman-Mackey, D., Agol, E., Ambikasaran, S., Angus, R.: Fast and scalable gaussian process modeling with applications to astronomical time series. *The Astronomical Journal* **154**(6), 220 (2017)
4. HajiGhassemi, N., Deisenroth, M.: Analytic Long-Term Forecasting with Periodic Gaussian Processes. In: Kaski, S., Corander, J. (eds.) *Proceedings of the Seventeenth International Conference on Artificial Intelligence and Statistics. Proceedings of Machine Learning Research*, vol. 33, pp. 303–311. PMLR, Reykjavik, Iceland (22–25 Apr 2014), <https://proceedings.mlr.press/v33/hajighassemi14.html>
5. Hensman, J., Fusi, N., Lawrence, N.D.: Gaussian processes for big data. arXiv preprint arXiv:1309.6835 (2013)
6. Li, Y., Zhang, Y., Xiao, Q., Wu, J.: Quasi-periodic gaussian process modeling of pseudo-periodic signals. *IEEE Transactions on Signal Processing* **71**, 3548–3561 (2023). <https://doi.org/10.1109/TSP.2023.3316589>
7. Nicholson, B.A., Aigrain, S.: Quasi-periodic gaussian processes for stellar activity: From physical to kernel parameters. *Monthly Notices of the Royal Astronomical Society* **515**(4), 5251–5266 (2022)
8. Paciorek, C.J., Schervish, M.J.: Nonstationary covariance functions for gaussian process regression. In: *Proceedings of the 17th International Conference on Neural Information Processing Systems*. p. 273–280. NIPS’03, MIT Press, Cambridge, MA, USA (2003)
9. Sańnick, O., Rosenstatter, T., Unterweger, A., Huber, S.: Deep learning-based time series forecasting for industrial discrete process data. In: *8th IEEE Conference on Industrial Cyber-Physical Systems (ICPS)*. IEEE, Emden, Germany (05 2025). <https://doi.org/10.1109/ICPS65515.2025.11087869>
10. Schindler, S., Reich, E.S., Messineo, S., Huber, S.: Topology-driven identification of repetitions in multi-variate time series. In: *Proceedings of the 6th Interdisciplinary Data Science Conference – iDSC2025* (2025), <https://arxiv.org/abs/2505.10004>

11. Solin, A., Särkkä, S.: Explicit Link Between Periodic Covariance Functions and State Space Models. In: Kaski, S., Corander, J. (eds.) Proceedings of the Seventeenth International Conference on Artificial Intelligence and Statistics. Proceedings of Machine Learning Research, vol. 33, pp. 904–912. PMLR, Reykjavik, Iceland (22–25 Apr 2014), <https://proceedings.mlr.press/v33/solin14.html>
12. Song, Y., Sohl-Dickstein, J., Kingma, D.P., Kumar, A., Ermon, S., Poole, B.: Score-based generative modeling through stochastic differential equations. arXiv preprint arXiv:2011.13456 (2020)
13. Titsias, M.: Variational learning of inducing variables in sparse gaussian processes. In: van Dyk, D., Welling, M. (eds.) Proceedings of the Twelfth International Conference on Artificial Intelligence and Statistics. Proceedings of Machine Learning Research, vol. 5, pp. 567–574. PMLR, Hilton Clearwater Beach Resort, Clearwater Beach, Florida USA (16–18 Apr 2009), <https://proceedings.mlr.press/v5/titsias09a.html>
14. Williams, C.K., Rasmussen, C.E.: Gaussian processes for machine learning. MIT Press: Cambridge, MA, USA (2006)

## Appendix

### 5.1 Proof of Property 1

*Proof.* We consider repeated noisy observations of a single latent function  $f \sim \mathcal{GP}(0, k)$  observed on a fixed grid of size  $n$ . With a periodic kernel, the embedding on the circle will provide this grid automatically, assuming all repetitions are phase aligned sequences of samples at equidistant times covering one period length  $p$  of the kernel. For repetitions  $i = 1, \dots, r$

$$y_i = f + \epsilon_i, \quad \epsilon_i \sim \mathcal{N}(0, \sigma^2 I)$$

The joint density of all repetitions is a block matrix with the observation noise  $\sigma^2$  added to its diagonal.

$$[y_1, \dots, y_r]^\top \sim \mathcal{N}(\mathbf{0}, \Sigma_r)$$

$$\Sigma_r = \begin{bmatrix} K + \sigma^2 I_n & K & \cdots & K \\ K & K + \sigma^2 I_n & \cdots & K \\ \vdots & \vdots & \ddots & \vdots \\ K & K & \cdots & K + \sigma^2 I_n \end{bmatrix}$$

With an  $r$ -dimensional vector  $\mathbb{1}_r$  of all ones and the Kronecker product  $\otimes$ , we can rewrite the matrix as

$$\begin{aligned} &= (\mathbb{1}_r \mathbb{1}_r^\top) \otimes K + \sigma^2 I_{nr}. \\ &= \underbrace{(\mathbb{1}_r \otimes I_n)}_U \underbrace{K}_C \underbrace{(\mathbb{1}_r \otimes I_n)^\top}_{U^\top} + \underbrace{\sigma^2 I_{nr}}_A. \end{aligned}$$

Recall the Woodbury identity

$$(UCV + A)^{-1} = A^{-1} - A^{-1}U(C^{-1} + VA^{-1}U)^{-1}VA^{-1},$$

which we apply as

$$(UCU^\top + A)^{-1} = A^{-1} - A^{-1}U(C^{-1} + U^\top A^{-1}U)^{-1}U^\top A^{-1}.$$

so we find the inverse of  $\Sigma_r$  by applying this identity twice:

$$\begin{aligned} \Sigma_r^{-1} &= \sigma^{-2}I_{nr} - \sigma^{-4}U(I_n K^{-1}I_n + \frac{r}{\sigma^2}I_n)^{-1}U^\top. \\ \Sigma_r^{-1} &= \sigma^{-2}I_{nr} - \sigma^{-4}(\mathbb{1}_r \mathbb{1}_r^\top) \otimes \underbrace{\left( \underbrace{I_n}_U \underbrace{K^{-1}}_C \underbrace{I_n}_{U^\top} + \underbrace{\frac{r}{\sigma^2}I_n}_A \right)^{-1}}_A \\ &= \sigma^{-2}I_{nr} - (\mathbb{1}_r \mathbb{1}_r^\top) \otimes \underbrace{\left( \frac{\sigma^{-2}}{r}I_n - \frac{1}{r^2}(K + \frac{\sigma^2}{r}I_n)^{-1} \right)}_A. \end{aligned}$$

The posterior mean on the grid then is

$$\begin{aligned} \hat{\mu} &= (\mathbb{1}_r^\top \otimes K) \Sigma_r^{-1} \begin{bmatrix} y_1 \\ \vdots \\ y_r \end{bmatrix} = [K \dots K] \begin{bmatrix} \sigma^{-2}y_1 - \sum_{j=1}^r \Lambda y_j \\ \vdots \\ \sigma^{-2}y_r - \sum_{j=1}^r \Lambda y_j \end{bmatrix} \\ &= \sum_{i=1}^r \sigma^{-2}K y_i - r \sum_{j=1}^r K \Lambda y_j = K (\sigma^{-2}I_n - r\Lambda) \sum_{i=1}^r y_i \\ &= K \left( K + \frac{\sigma^2}{r}I_n \right)^{-1} \frac{1}{r} \sum_{i=1}^r y_i. \end{aligned} \tag{12}$$

Conditioning a GP on multiple noisy observations of the same underlying latent function is equivalent to conditioning on the mean observation and reducing the observation uncertainty  $\sigma^2$  by a factor of the number of observations  $\frac{1}{r}$ . Without observation uncertainty ( $\sigma \rightarrow 0$ ) or in the limit of infinitely many observations ( $r \rightarrow \infty$ ), the posterior predictive mean converges to the expected observation. With the same approach, one can also find the posterior covariance matrix which also simplifies nicely, leaving one with the same scaled variance as in the expression for the mean

$$\hat{\Sigma} = K - K \left( K + \frac{\sigma^2}{r}I_n \right)^{-1} K. \tag{13}$$

This reduction of effective observation variance explains why increasing the number of repetitions sharpens the posterior and decreases predictive variability.